



ELSEVIER

Nuclear Physics A698 (2002) 408c–411c

[www.elsevier.com/locate/npe](http://www.elsevier.com/locate/npe)

## The STAR Time Projection Chamber

F. Retière <sup>a</sup> for the STAR collaboration \*

<sup>a</sup>Lawrence Berkeley National Laboratory

The STAR Time Projection Chamber was successfully operated during the first RHIC run in 2000. Most of the STAR contributions reported in these proceedings are based on the analysis of data from the TPC. In this article, we show that the performance achieved by the TPC, in terms of track reconstruction, position resolution, and particle identification are well suited for measuring precise and reliable physics observables.

### 1. Introduction

The STAR experiment is a large acceptance detector dedicated to the study of relativistic heavy ion collisions at RHIC. The Time Projection Chamber covers a wide acceptance range :  $|\eta| < 1.8$ ,  $p_t > 100 \text{ MeV}/c$  and  $0 < \phi < 2\pi$ . It sits inside a 0.25 Tesla solenoidal magnet which can be operated up to 0.5 Tesla. Particle identification is achieved by measuring the energy loss, applying topological cuts [1] or constructing invariant masses [2]. The TPC is 4 meters in diameter and 4.2 meters long. It is filled with a mixture of 90% argon and 10% methane and is shown schematically in figure 1. The tracking volume is surrounded by an electrostatic field cage which is built with 11.5 mm wide rings to divide the voltage from -31 kV on the central membrane to 0 V on the ground wires. The field cages are very thin : 0.62% radiation length for the inner field cage and 1.26% radiation length for the outer field cage.

Each side of the TPC is segmented into 12 azimuthal sectors. One sector is shown in figure 2. The figure includes a cross sectional view of the wire layers and pad plane. There are three layers of wires terminating each side of the chamber. The first layer is the gating grid which terminates the field cage voltage and is used to close the chamber when no trigger is detected. The second layer is the ground plane which captures the ions from the amplification region and the third layer is the anode plane. Gas amplification is achieved around each anode wire and the induced signal is picked up on the pad plane located under the anode wires.

Each sector is divided into an inner and an outer part. The inner sector has 1,750 pads, each 2.85 mm wide (tangential direction) and 11.5 mm high (radial direction). They are grouped into 13 pad rows located between 60 cm and 116 cm from the beam line. The outer sector has 3,940 pads which are 6.2 mm wide and 19.5 mm high. The outer sector covers 32 pad rows between 127.2 cm and 189.1 cm radius. In order to keep the signal to noise ratio constant at 20:1 for both size pads, the anode voltages were set to achieve a gain of 1230 on the outer sector and 3760 on the inner sector.

\* Author list given in [5]

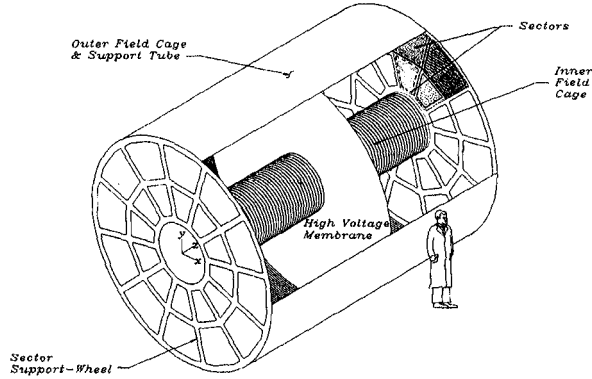


Figure 1. A schematic view of the TPC : showing the electrostatic field cage, the cathode in the middle, and the read-out pad planes on either end.

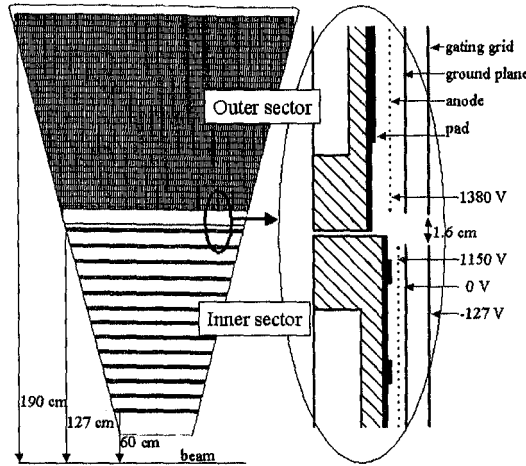


Figure 2. The read-out pad plane geometry. Left : top view of the pad plane. Right : side view of the pad plane including the wire planes labelled on the figure.

The signal measured on the pads is amplified using custom CMOS ICs[3]. The arrival time of the electrons is sampled and read out into 512 time bins using a Switched Capacitor Array and ADC. The position of the particle along the drift direction is then reconstructed by converting from time bin to position by knowing the drift velocity. For a more complete description of the TPC see [4]. In the next section we will show that we understand the systematic errors that affect the position resolution. We will conclude with a study of the  $dE/dx$  resolution which is affected by gain and ionization fluctuations.

## 2. Position reconstruction

The position resolution in the TPC has been extensively studied using cosmic rays and Au+Au data. A resolution of  $500\ \mu\text{m}$  along the pad row is achieved, for example, with straight tracks in the inner sector. We have achieved a momentum resolution of 2% for

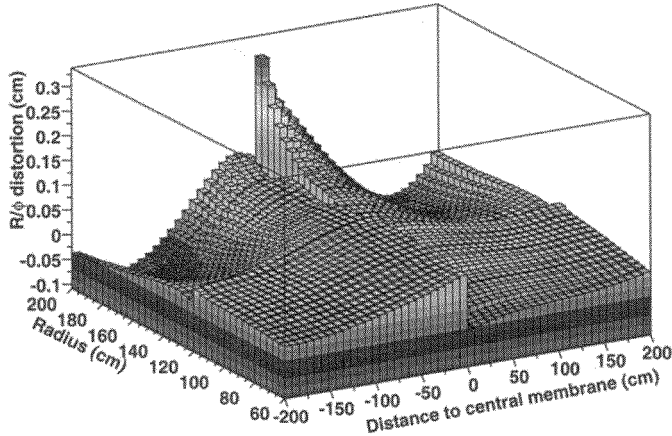


Figure 3. Distortion along the pad row as a function of the pad row number and the distance along the beam axis.

pions at 500 MeV/c.

Ideally, ionization electrons drift toward the TPC endcaps along straight lines. However, detector imperfections modify their trajectories and introduce systematic errors in the measured positions. In the STAR TPC these deviations are identified using position survey data and magnetic field maps. We then calculate the magnitude of the distortions without using any adjustable parameters. The sum of all known distortions is shown in figure 3. The maximum amplitude of these distortions is a few mm. The effect of the distortions is also clearly shown in the residual difference between the fitted track position on the pad row and the true hit position measured on this pad row. The maximum average residual is significantly reduced after correcting the data for the calculated distortions. The coordinate along the beam axis is obtained from the measured drift times of the electrons by knowing the electron drift velocity. This velocity is precisely measured by calculating the difference between the known position of several laser beams shining inside the TPC. The drift velocity was further constrained by matching both primary vertexes found using tracks from each side of the TPC, independently. The measured dependence of the drift velocity with pressure and methane content agrees well with theoretical estimates.

### 3. Particle identification capabilities

In the TPC, particles coming from the primary vertex are identified by measuring their energy loss in the gas volume. Our ability to separate the different particle species is strongly dependent on the  $dE/dx$  resolution. Ionization and gain fluctuations have to be understood and minimized. The statistical fluctuations are partly cancelled out by averaging over a large enough number of samples, i.e. in STAR, up to 45 points. The systematic fluctuations are due to gain non-uniformity; gas gain variation with time, and gas and electronic variation over the TPC. The gas gain variation with time is monitored by averaging the  $dE/dx$  measured over the whole TPC. We found that the gas gain is

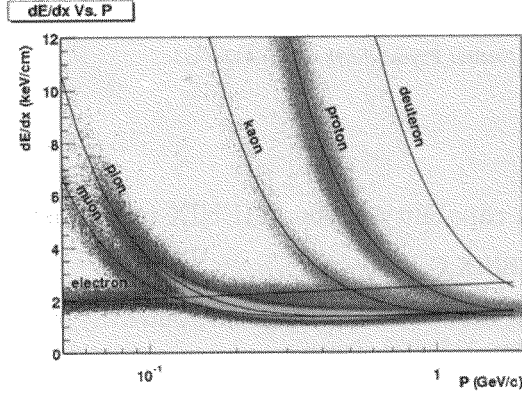


Figure 4. Energy loss measured in the STAR TPC

most sensitive to barometric pressure variations.

To correct for gain variation over the TPC, gain coefficients are applied to each pad. Average  $dE/dx$  values are calculated for each pad row. A gain coefficient is extracted for each row in order to correct for the gain variations on each row with respect to the others. Indeed, the gas gain could vary from wire to wire (which mean from pad row to pad row because the wires are parallel to the pad rows). There are additional pad by pad  $dE/dx$  fluctuations which are due to gain variations in the readout electronics. These fluctuations are corrected by pulsing the ground plane with a pulser inducing the same signal on every pad. A few hundred events are sufficient to extract precise electronic gain correction coefficients.

Gain calibration improves the  $dE/dx$  resolution significantly. After calibration, protons can be separated from pions up to a momentum of 1.3 GeV as shown on figure 4. Low momentum muons can also be identified in between the pion and electron bands.

#### 4. Conclusions

The STAR TPC has nearly reached its design and performance specifications. Momentum resolution of 2% at a reference  $p_t$  of 500 MeV/c has been achieved while protons and pions can be separated using  $dE/dx$  at a momentum up to 1.3 GeV/c. These performance parameters combined with the large acceptance of the TPC allowed the STAR collaboration to contribute significantly to this quark matter conference (see [5] for an overview).

#### REFERENCES

1. H. Caines for the STAR collaboration, these proceedings
2. Z. Chu for the STAR collaboration, these proceedings
3. S.Klein, et al., IEEE Trans Nucl. Sci. 43 (1996) 1768
4. K. Ackermann, et al., Nucl. Phys. A661 (1999) 686c, and CDR, LBL Pub-5347 (1992)
5. J. Harris for the STAR collaboration, these proceedings